J-Matrix Analysis of Resonant States in the Shell Model

A. I. Mazur[a], A. M. Shirokov[a,b,c], J. P. Vary[c], P. Maris[c] and I. A. Mazur[a]

[a] *Department of Physics, Pacific National University, Khabarovsk 680035, Russia*
[b] *Skobeltsyn Institute of Nuclear Physics, Lomonosov Moscow State University, Moscow 119991, Russia*
[c] *Department of Physics and Astronomy, Iowa State University, Ames, Iowa 50011, USA*

Abstract

We suggest a method for calculating scattering phase shifts and energies and widths of resonances which utilizes only eigenenergies obtained in variational calculations with oscillator basis and their dependence on oscillator basis spacing $\hbar\Omega$. The validity of the suggested approach is verified in calculations with model Woods–Saxon potentials and applied to calculations of resonances in $n\alpha$ scattering using the no-core shell model.

Keywords: *Shell model; J-matrix approach; resonance energy and width; Breit–Wigner resonance formula; $n\alpha$ scattering*

1 Introduction

To calculate energies of nuclear ground states and other bound states within various shell model approaches, one conventionally starts by calculating the $\hbar\Omega$-dependence of the energy $E_\nu(\hbar\Omega)$ of the bound state ν in some model space. The minimum of $E_\nu(\hbar\Omega)$ is correlated with the energy of the state ν. The convergence of calculations and accuracy of the energy prediction is estimated by comparing with the results obtained in neighboring model spaces. To improve the accuracy of theoretical predictions, various extrapolation techniques have been suggested recently [1, 2, 3, 4] which make it possible to estimate the binding energies in the complete infinite shell-model basis space.

Is it possible to study nuclear states in the continuum, resonant states in particular, in the shell model using bound state techniques? A conventional belief is that the energies of shell-model states in the continuum should be associated with the resonance energies. It was shown however in Ref. [5] that the energies of shell-model states may appear well above the energies of resonant states, especially for broad resonances. Moreover, the analysis of Ref. [5] clearly demonstrated that the shell model should also generate some states in a non-resonant nuclear continuum. The nuclear resonance properties can be studied in the Gamow shell model, including the *ab initio* no-core Gamow shell model (NCGSM) [6]. Another option is to combine the shell model with resonating group method (RGM). An impressive progress in description of various nuclear reactions was achieved by means of the combined no-core shell model/RGM (NCSM/RGM) approach [7]. Both NCGSM and NCSM/RGM complicate essentially the shell model calculations. Is it possible to get some information about the unbound nuclear states directly from the results of calculations in NCSM or other versions of the nuclear shell model without introducing additional Berggren basis states as in NCGSM or additional RGM calculations as in the NCSM/RGM approach?

A complete study of the nuclear continuum can be performed by extending the nuclear shell model by J-matrix formalism in scattering theory. The J-matrix formalism

has been suggested in atomic physics [8, 9]. Later it was independently rediscovered in nuclear physics [10, 11] and was successfully used in shell-model applications [12]. However a direct implementation of the J-matrix formalism in modern large-scale shell-model calculations is very complicated: the J-matrix requires calculation of a huge number of eigenstates while modern shell-model codes usually utilize Lanczos algorithm which provides only few lowest Hamiltonian eigenstates. Furthermore, the J-matrix needs also the highest component of wave function of each eigenstate which is usually obtained with a low precision.

On the other hand, the J-matrix formalism can be used for a simple calculation of the scattering phase shift at a single energy $E_\nu(\hbar\Omega)$ which is an eigenstate of the shell-model Hamiltonian. In this case, the phase shift calculation requires only the value of the energy $E_\nu(\hbar\Omega)$ and the basis parameters (the $\hbar\Omega$ value and the basis size). Varying the shell-model parameter $\hbar\Omega$, we generate a variation of $E_\nu(\hbar\Omega)$ and hence we can calculate the phase shifts in some energy range. Calculations of scattering phase shifts at the eigenenergies of the Hamiltonian in the oscillator basis and obtaining the phase shift energy dependence by variation of basis parameters, was recently performed in Ref. [4] using another (not the J-matrix) technique. A detailed study of scattering phase shifts at eigenenergies of the Hamiltonian in arbitrary finite $\mathcal{L}^2$ basis was performed in Ref. [13]. This study was based on the theory of spectral shift functions introduced by I. M. Lifshitz more than 60 years ago [14] and later forgotten by physicists though used up to now by mathematicians (see Ref. [13] and references therein).

In this contribution, we study the behavior of scattering phase shifts at the eigenenergies $E_\nu(\hbar\Omega)$ of the Hamiltonian in the oscillator basis. Our aim is to formulate criteria for selecting eigenstates associated with resonances and to develop an approach to evaluating energies and widths of these resonances. We are using the J-matrix formalism which provides exact phase shifts in the systems with potential energy described by a finite matrix in oscillator basis, i. e., just in the case of the nuclear shell model.

A brief sketch of the J-matrix theory and examples of phase shift calculations with model interactions are presented in the next Section. Application of the approach to calculations of phase shifts at the eigenenergies $E_\nu(\hbar\Omega)$ of the Hamiltonian in the oscillator basis, comparison with the spectral shift function theory of I. M. Lifshitz and criteria for selecting eigenstates associated with resonances are discussed in Section 3. In Section 4, we discuss the relation between the parameters of the Breit–Wigner resonance formula and the $\hbar\Omega$ dependence of the eigenenergy $E_\nu(\hbar\Omega)$ and give examples of calculating Breit–Wigner parameters with model interactions. An analysis of resonance energies and widths in neutron-α scattering based on NCSM calculations of ^{5}He nucleus is presented in Section 5.

2 *J*-matrix formalism

We discuss here the simplest version of the J-matrix formalism — a single-channel elastic scattering of an uncharged particle. We use notations of Refs. [15, 16] where one can find more details of the J-matrix theory, the multi-channel version of this approach, a technique of accounting for the long-range Coulomb interaction, etc.

The radial wave function $u_l(k,r)$ describing the relative motion in the partial wave with orbital momentum l is expanded in the J-matrix formalism in infinite series of radial oscillator functions $R_{nl}(r)$,

$$u_l(k,r) = \sum_{n=0}^{\infty} a_{nl}(k)\, R_{nl}(r), \tag{1}$$

where

$$R_{nl}(r) = (-1)^n \sqrt{\frac{2n!}{r_0\,\Gamma(n+l+3/2)}} \left(\frac{r}{r_0}\right)^{l+1} \exp\left(-\frac{r^2}{2r_0^2}\right) L_n^{l+\frac{1}{2}}\left(\frac{r^2}{r_0^2}\right). \qquad (2)$$

Here k is the relative motion momentum, $L_n^\alpha(z)$ are Laguerre polynomials and n is the harmonic oscillator radial quantum number. Using expansion (1) we transform the radial Schrödinger equation

$$H^l\, u_l(k,r) = E\, u_l(k,r) \qquad (3)$$

into an infinite set of linear algebraic equations

$$\sum_{n'=0}^{\infty} (H^l_{nn'} - \delta_{nn'}E) a_{n'l}(k) = 0, \qquad (4)$$

where $H^l_{nn'} = T^l_{nn'} + V^l_{nn'}$ are matrix elements of the Hamiltonian H^l in the oscillator basis, and $T^l_{nn'}$ and $V^l_{nn'}$ are kinetic and potential energy matrix elements respectively.

The kinetic energy matrix elements $T^l_{nn'}$ are known to form a tridiagonal matrix, i. e., the only non-zero matrix elements are

$$\begin{aligned} T^l_{nn} &= \frac{1}{2}\hbar\Omega(2n+l+3/2), \\ T^l_{n,n+1} &= T^l_{n+1,n} = -\frac{1}{2}\hbar\Omega\sqrt{(n+1)(n+l+3/2)}. \end{aligned} \qquad (5)$$

These matrix elements are seen to increase linearly with n for large n. On the other hand, the potential energy matrix elements $V^l_{nn'}$ decrease as $n, n' \to \infty$. Hence the kinetic energy dominates in the Hamiltonian matrix at large enough n and/or n'. Therefore a reasonable approximation is to truncate the potential energy matrix at large n and/or n', i. e., to approximate the interaction V by a nonlocal separable potential $\tilde{V}$ with matrix elements

$$\tilde{V}^l_{nn'} = \begin{cases} V^l_{nn'} & \text{if} \quad n \le N \text{ and } n' \le N; \\ 0 & \text{if} \quad n > N \text{ or } n' > N. \end{cases} \qquad (6)$$

The approximation (6) is the only approximation in the J-matrix approach; for separable interactions of the type (6), the J-matrix formalism suggests exact solutions. Note, the kinetic energy matrix is not truncated in the J-matrix theory contrary to conventional variational approaches like the shell model.

The complete infinite harmonic oscillator basis space can be divided into two subspaces according to truncation (6): an internal subspace spanned by oscillator functions with $n \le N$ where the interaction V is accounted for and an asymptotic subspace spanned by oscillator functions with $n > N$ associated with the free motion.

Algebraic equations (4) in the asymptotic subspace take the form of a second order finite-difference equation:

$$T^l_{nn-1}\, a^{ass}_{n-1l}(E) + (T^l_{nn} - E)\, a^{ass}_{nl}(E) + T^l_{nn+1}\, a^{ass}_{n+1l}(E) = 0. \qquad (7)$$

Any solution $a^{ass}_{nl}(E)$ of Eq. (7) can be expressed as a superposition of regular $S_{nl}(E)$ and irregular $C_{nl}(E)$ solutions,

$$a^{ass}_{nl}(E) = \cos\delta_l\, S_{nl}(E) + \sin\delta_l\, C_{nl}(E), \quad n \ge N, \qquad (8)$$

where δ_l is the scattering phase shift. The solutions $S_{nl}(E)$ and $C_{nl}(E)$ have simple analytical expressions [9, 11, 15]:

$$S_{nl}(E) = \sqrt{\frac{\pi n!}{\Gamma(n+l+3/2)}}\, q^{l+1} \exp\left(-\frac{q^2}{2}\right) L_n^{l+1/2}(q^2), \qquad (9)$$

$$C_{nl}(E) = (-1)^l \sqrt{\frac{\pi n!}{\Gamma(n+l+3/2)}}\, \frac{q^{-l}}{\Gamma(-l+1/2)} \times \exp\left(-\frac{q^2}{2}\right) \Phi(-n-l-1/2, -l+1/2; q^2), \quad (10)$$

where $\Phi(a, b; z)$ is a confluent hypergeometric function and q is a dimensionless momentum,

$$q = \sqrt{\frac{2E}{\hbar\Omega}}. \quad (11)$$

The solutions $a_{nl}(E)$ of the algebraic set (4) in the internal subspace $n \leq N$ are related to the solutions $a^{ass}_{nl}(E)$ in the asymptotic subspace $n \geq N$:

$$a_{nl}(E) = \mathcal{G}_{nN}\, T^l_{N,N+1}\, a^{ass}_{N+1,\,l}(E). \quad (12)$$

Here matrix elements

$$\mathcal{G}_{nn'} = -\sum_{\nu=0}^{N} \frac{\langle n|\nu\rangle\langle\nu|n'\rangle}{E_\nu - E} \quad (13)$$

are related to the Green's function of the Hamiltonian H^N which is the Hamiltonian H^l truncated to the internal subspace, and are expressed through eigenenergies E_ν and eigenvectors $\langle n|\nu\rangle$ of the Hamiltonian H^N:

$$\sum_{n'=0}^{N} H^l_{nn'}\langle n'|\nu\rangle = E_\nu\langle n|\nu\rangle, \quad n \leq N. \quad (14)$$

A relation for calculation of the scattering phase shifts δ_l can be obtained through the matching condition

$$a_{Nl}(E) = a^{ass}_{Nl}(E). \quad (15)$$

Using Eqs. (8), (12) and (15) it is easy to obtain [9, 11, 15]

$$\tan\delta_l(E) = -\frac{S_{Nl}(E) - \mathcal{G}_{NN}\, T^l_{N,N+1}\, S_{N+1,l}(E)}{C_{Nl}(E) - \mathcal{G}_{NN}\, T^l_{N,N+1}\, C_{N+1,l}(E)}. \quad (16)$$

The scattering phase shifts $\delta_l(E)$ can be calculated using Eq. (16). An acceptable range of J-matrix parameters (ARJP) $\hbar\Omega$ and N where the scattering phase shifts $\delta_l(E)$ can be calculated with a reasonable precision, depends on the potential V. The convergence of phase shift calculations can be improved, and hence the ARJP can be enlarged, by 'smoothing' the potential truncation in the oscillator basis space, i. e., by replacing the matrix elements (6) by [17]

$$\mathcal{V}_{nn'} = \sigma^n_N\, \widetilde{V}_{nn'}\, \sigma^{n'}_N, \quad (17)$$

where

$$\sigma^n_N = \frac{1 - \exp\{-[\alpha(n-N-1)/(N+1)]^2\}}{1 - \exp(-\alpha^2)}. \quad (18)$$

We employ the smoothing (17)–(18) with the parameter $\alpha = 5$ in our calculations with model interactions presented below.

We illustrate the J-matrix calculations of the phase shifts in the vicinity of resonances in Fig. 1. We use a model Woods–Saxon potential with surface repulsion generating a resonance,

$$V(r) = V_0 \frac{1}{1+z} + V_s \frac{b}{r}\frac{z}{(1+z)^2}, \quad (19)$$

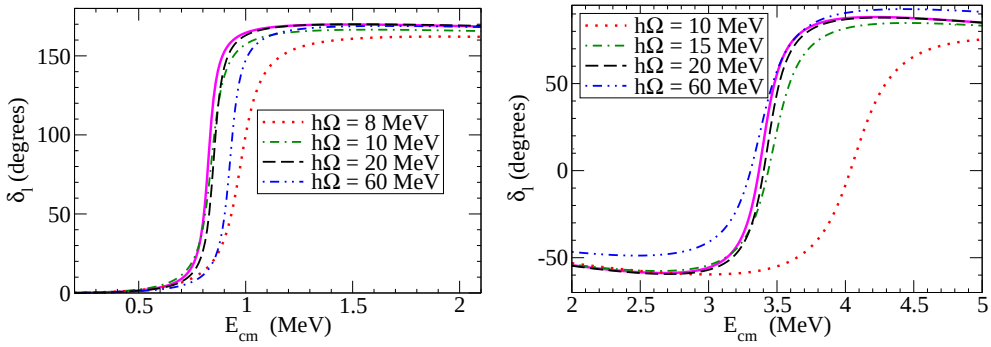

Figure 1: d wave (left) and s wave (right) phase shifts in the vicinity of resonances calculated with model interactions (19) in the J-matrix approach with $N = 5$ and various $\hbar\Omega$ values. The exact phase shifts generated by these interactions are depicted by solid lines.

Table 1: Parameters of the model Woods–Saxon potentials (19) in d and s waves and energies E_r and widths Γ of resonances generated by these potentials.

Partial wave	L	V_0 (MeV)	V_s (MeV)	R (fm)	a (fm)	b (fm)	E_r (MeV)	Γ (MeV)
d	2	−48.0	−20.0	3.08	0.53	3.774	0.8319	0.0612
s	0	−50.0	207.0	3.08	0.53	3.774	3.403	0.2250

where

$$z = \exp\left(\frac{r-R}{a}\right). \tag{20}$$

The reduced mass $m = \frac{4}{5}m_n$ (m_n is a nucleon mass) was used in calculations that corresponds to the scattering of neutron by α-particle. The parameters of the interaction (19) and energies and widths of model resonances generated by it in s and d waves, are presented in Table 1.

The phase shift calculations are well-converged for $N = 5$ in the interval of $\hbar\Omega$ values ranging between 25 and 40 MeV where the J-matrix phase shifts are indistinguishable from the exact results depicted by solid curves in Fig. 1. If $\hbar\Omega$ is taken outside this interval, the J-matrix phase shifts differ from exact as is seen in Fig. 1. The interval of $\hbar\Omega$ values providing excellent description of the phase shifts expands when the truncation boundary N increases. For example, the interval of acceptable $\hbar\Omega$ values starts from approximately 15 MeV in case of $N = 10$.

3 Phase shift and its derivative at $E = E_\nu$

When the energy of relative motion E is equal to one of eigenenergies E_ν of the truncated Hamiltonian H^N, expression (16) for calculation of the phase shifts transforms into

$$\tan\delta_l(E_\nu) = -\frac{S_{N+1,l}(E_\nu)}{C_{N+1,l}(E_\nu)}. \tag{21}$$

The eigenenergy E_ν depends on the size of the internal basis space N and on the value of the oscillator spacing $\hbar\Omega$, $E_\nu = E_\nu(N, \hbar\Omega)$. Therefore one can use Eq. (21) to calculate the phase shifts $\delta(E)$ in some interval of energies E ranging from $E_\nu(\hbar\Omega_1)$ through $E_\nu(\hbar\Omega_2)$ by varying $\hbar\Omega$ within ARJP from $\hbar\Omega_1$ through $\hbar\Omega_2$. The values

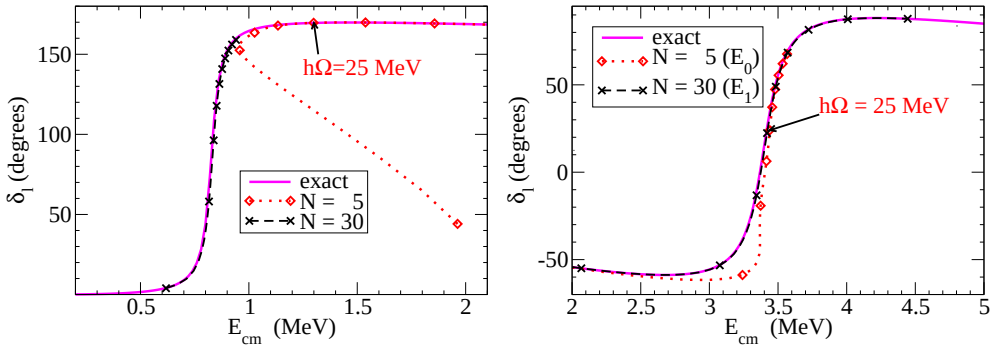

Figure 2: d wave (left) and s wave (right) phase shifts in the vicinity of resonances calculated with model interactions (19) at the eigenenergies of the truncated Hamiltonian H^N by means of Eq. (21) with $N = 5$ and 30 and various $\hbar\Omega$. The lowest $\hbar\Omega$ value within ARJP in case of $N = 5$ truncation is $\hbar\Omega_1 \approx 25$ MeV, the respective points on the phase shift curves are indicated.

of the lower $\hbar\Omega_1$ and upper $\hbar\Omega_2$ ARJP bounds depend, of course, on N and generally speaking are different for different states $\nu = 0, 1, 2, ...$ If the ARJP is wide enough and the energy interval $[E_\nu(\hbar\Omega_1), E_\nu(\hbar\Omega_2)]$ covers completely the vicinity of the resonance, the resonance parameters are easily restored from the phase shift behavior in this energy interval. In this case the resonance parameters can be calculated through the $\hbar\Omega$-dependence of eigenenergy $E_\nu = E_\nu(\hbar\Omega)$ obtained in a standard variational calculation with oscillator basis. However, in some cases the energy interval $[E_\nu(\hbar\Omega_1), E_\nu(\hbar\Omega_2)]$ covers only a fraction, sometimes, a small fraction of the energy range of the resonant behavior of the phase shifts. In those cases, the extraction of the resonance energy and width is more complicated and less accurate. More, sometimes the energy interval $[E_\nu(\hbar\Omega_1), E_\nu(\hbar\Omega_2)]$ corresponds to a non-resonant scattering as was clearly demonstrated in Ref. [5].

We demonstrate in Fig. 2 calculations of phase shifts by means of Eq. (21) in the vicinity of resonances generated in s and d waves by model interactions (19). In the case of d wave, calculations with $N = 5$ and 30 are performed with the lowest eigenstate ($\nu = 0$) obtained with $\hbar\Omega$ ranging from 2.5 to 50 MeV. In the case of s wave, varying $\hbar\Omega$ in the same interval from 2.5 to 50 MeV in calculations with $N = 5$, we obtain the variation of the lowest eigenstate energy E_0 between 0.64 and 3.57 MeV covering the vicinity of the resonance. However in calculations with $N = 30$, the lowest eigenstate energy E_0 varies from 0.11 to 3.15 MeV due to variation of $\hbar\Omega$ in the same interval, i. e., E_0 lies below the resonance region. The vicinity of the resonance in this case is completely covered by variation of the energy E_1 of the next state with $\nu = 1$, and we use E_1 for calculations of the phase shifts in the resonance region. We obtain an excellent description of the phase shifts if the J-matrix parameters are lying within ARJP. However when $\hbar\Omega$ goes outside ARJP, the obtained phase shifts start deviating from the exact ones. This deviation can be very large when $\hbar\Omega$ is far enough from ARJP and the phase shifts may become ambiguous in some energy interval due to unphysical 'backbending' energy dependence (see the left panel of Fig. 2) obtained by variation of $\hbar\Omega$ far outside ARJP.

It is interesting to compare the J-matrix approach to calculations of phase shifts at eigenenergies E_ν with the approach utilizing the spectral shift functions of I. M. Lifshitz [14]. We note that the phase shifts at eigenenergies E_ν due to Eq. (21) are equal to

$$\delta_l(E_\nu) = f_{N+1,l}(E_\nu) + m\pi, \tag{22}$$

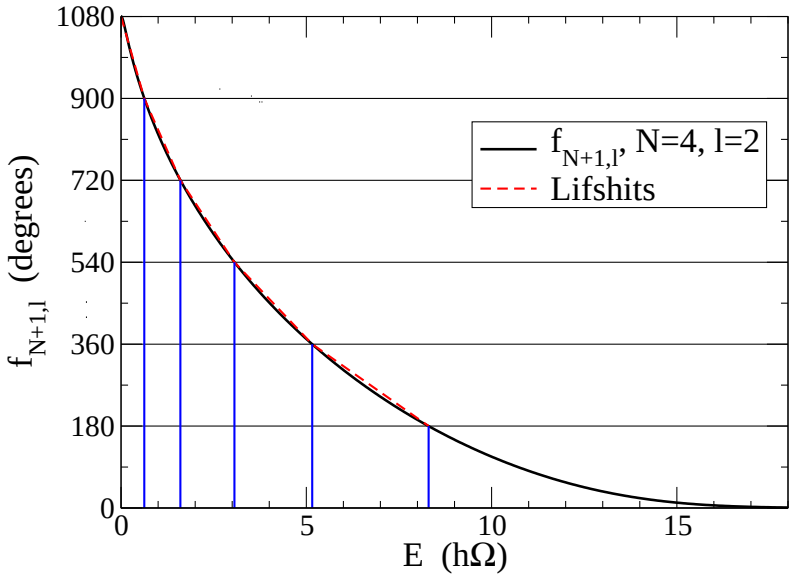

Figure 3: Universal function $f_{N+1,l}(E)$ in case of $N = 4$ and $l = 2$ and its approximation in the Lifshitz spectral shift function method. The vertical solid lines correspond to eigenenergies E^0_ν) of the truncated kinetic energy T^N.

where m can be zero or takes some positive or negative integer value, and the function

$$f_{nl}(E) = -\arctan\left(\frac{S_{nl}(E)}{C_{nl}(E)}\right). \tag{23}$$

Due to Eqs. (9), (10) and (23), it is clear that $f_{nl}(E)$ depends on the energy E and $\hbar\Omega$ only in combination $E/\hbar\Omega$. $f_{nl}(E)$ is a monotonically decreasing function of a dimensionless energy $\varepsilon = E/\hbar\Omega$ which goes down by $(n+1)\pi$ as ε increases from 0 to infinity. An example of this function corresponding to the case $n = 5$ and $l = 2$ is presented in Fig. 3. The values of the function $f_{N+1,l}(E_\nu)$ provide the J-matrix phase shift δ_l at the eigenenergy E_ν for a given $\hbar\Omega$ value as is shown in Fig. 4 where we present in a larger scale a piece of the function $f_{N+1,l}(E)$ shifted to the interval of its values $[0, \pi]$ [the shift of this function by $m\pi$ is of no importance since we can always redefine m in Eq. (22)].

Within the Lifshitz spectral shift function approach [14, 13], the phase shift is calculated as

$$\delta_l(E_\nu) = -\pi\frac{E_\nu - E^0_\nu}{E^0_{\nu+1} - E^0_\nu}. \tag{24}$$

Here E_ν are the eigenvalues of the truncated Hamiltonian H^N while E^0_ν are the eigenvalues of the kinetic energy T^N truncated to the matrix of the same size as H^N. We recall that the kinetic energy has a tridiagonal matrix (5) in the oscillator basis, the functions $S_{nl}(E)$ are regular solutions of the respective finite-difference equation (7), and the eigenenergies E^0_ν of the truncated kinetic energy T^N can be obtained by solving this finite-difference equation with the boundary condition

$$S_{N+1,l}(E^0_\nu) = 0. \tag{25}$$

Therefore, due to Eq. (23), the kinetic energy eigenstates correspond to the energies at which $\tan f_{N+1,l}(E^0_\nu) = 0$ or when the function $f_{N+1,l}(E^0_\nu) = m\pi$, i. e., when the plot of the function $f_{N+1,l}(E)$ crosses the horizontal lines at π, 2π, ... as is shown in Fig. 3. We connect these crossing points by straight lines in Fig. 3. A set of these straight lines is seen to provide a good approximation for the function $f_{N+1,l}(E)$.

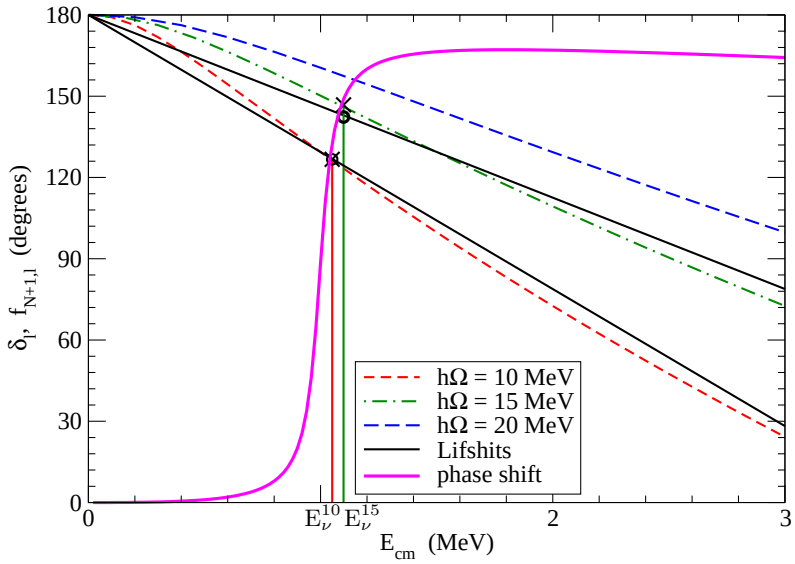

Figure 4: Calculation of phase shifts at eigenenergies E_ν in the J-matrix approach and using Lifshitz spectral shift function method. Dashed lines depict the function $f_{N+1,l}(E)$ for various $\hbar\Omega$ values, solid straight lines depict approximation of this function in the Lifshitz approach. E_ν^{10} and E_ν^{15} are eigenenergies obtained with $\hbar\Omega = 10$ and 15 MeV respectively. Crosses (circles) show the J-matrix (Lifshitz) phase shifts obtained with $\hbar\Omega = 10$ and 15 MeV, solid curve shows the J-matrix phase shifts in a continuous energy interval.

According to Eq. (24), the phase shifts at eigenenergies E_ν in the Lifshitz approach are obtained as the values of this straight-line approximation of the function $f_{N+1,l}(E)$ at energies E_ν as shown in Fig. 4.

It is seen that the J-matrix and Lifshitz approach provide close results for the phase shifts if N is large enough when the strait-line Lifshitz approximation of the function $f_{N+1,l}(E)$ is accurate. In Fig. 4, the difference of $\delta_l(E_\nu)$ values obtained by these approaches is the difference between positions of crosses and circles. It is interesting that the model interaction used to prepare this figure provides exactly the same phase shifts $\delta_l(E_\nu)$ for both methods in calculations with $\hbar\Omega = 10$ MeV. A comparison of results of calculations by means of these two approaches of phase shifts generated by our model interaction (19) in the d wave, is shown in Fig. 5.

It is also interesting to compare our J-matrix approach with the method of Ref. [4]

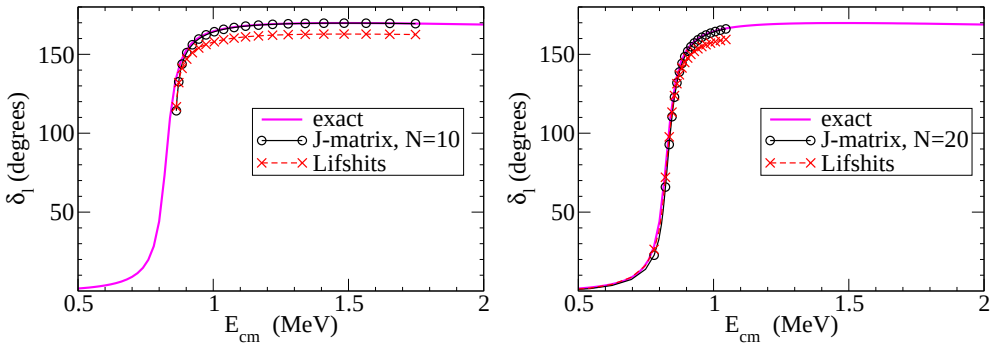

Figure 5: Comparison of d wave phase shifts obtained by J-matrix and Lifshitz methods for the model interaction (19) with $N = 10$ and 20.

where the phase shifts at the eigenenergies of the Hamiltonian H^N truncated in the oscillator basis was suggested to obtain through the following equation:

$$\tan\delta_l(E_\nu) = \frac{j_l(k_\nu L_i)}{n_l(k_\nu L_i)}. \tag{26}$$

Here $j_l(x)$ and $n_l(x)$ are spherical Bessel and Neumann functions, momentum $k_\nu = \sqrt{2mE_\nu/\hbar^2}$, and for low momenta

$$L_i = \sqrt{2(2N+l+3/2+i)}\, r_0, \tag{27}$$

$$r_0 = \sqrt{\frac{\hbar}{m\Omega}}. \tag{28}$$

The parameter L_i was involved in Ref. [4] in the study of convergence properties of bound states of the Hamiltonian H^N, and the best fit of convergence behavior resulted in $i = 2$.

Equation (26) can be easily obtained from our J-matrix formula (21) in the limit of large N. Asymptotics of functions $S_{nl}(E)$ and $C_{nl}(E)$ were studied in detail in Ref. [18]. In the limit of large n, more precisely, for $n \gg q$, the functions (9) and (10) are well approximated by spherical Bessel and Neumann functions [18, 15]:

$$S_{nl}(E) \approx 2kr_0(n+l/2+3/4)^{\frac{1}{4}}\, j_l\Big(2kr_0\sqrt{n+l/2+3/4}\Big), \tag{29}$$

$$C_{nl}(E) \approx -2kr_0(n+l/2+3/4)^{\frac{1}{4}}\, n_l\Big(2kr_0\sqrt{n+l/2+3/4}\Big). \tag{30}$$

Substituting $S_{nl}(E)$ and $C_{nl}(E)$ in Eq. (21) by their asymptotics (29) and (30), we immediately obtain Eq. (26). The value of $i = 2$ for the parameter L_i unambiguously follows from the fact that $S_{nl}(E)$ and $C_{nl}(E)$ appear in Eq. (21) with $n = N + 1$.

It is easy to conclude from Fig. 3 that eigenvalues E_ν lying in the vicinity of the resonance where the phase shift is rapidly increasing, should change only slightly when the value of $\hbar\Omega$ is changed and hence the derivative $\frac{dE_\nu}{\hbar d\Omega}$ should be small and positive. A wider resonance is associated with a less rapid increase of δ_l and a larger value of the derivative $\frac{dE_\nu}{\hbar d\Omega}$. One should be however accurate with making conclusions about the relative widths of resonances based on comparison of values of derivatives $\frac{dE_\nu}{\hbar d\Omega}$ of respective eigenvalues E_ν. First, the slope of the function $f_{N+1,l}(E)$ decreases with energy E and hence the derivatives $\frac{dE_\nu}{\hbar d\Omega}$ are different for the resonances of the same width but of different energy. Next, the slope of $f_{N+1,l}(E)$ depends also on the orbital momentum l and hence the derivatives $\frac{dE_\nu}{\hbar d\Omega}$ are different for the resonances of the same width and energy but of different l. It is also important to get the eigenvalue E_ν in the vicinity of the resonance: the derivative $\frac{dE_\nu}{\hbar d\Omega}$ decreases when the eigenvalue E_ν is shifted to the edge of the resonance region where the slope of $\delta_l(E)$ decreases; $\frac{dE_\nu}{\hbar d\Omega}$ gets even larger values in the non-resonant region.

Which eigenvalues E_ν are associated with a resonance and which are not? It is important to find a condition able to distinguish these eigenvalues. The phase shift $\delta_l(E)$ is increasing and hence the derivative $d\delta_l/dE$ is positive in the resonance region. We need to find an expression for $\delta_l(E)$ at the energies $E = E_\nu$. Using Eqs. (9) and (10) and expressions for the derivatives of Laguerre polynomials and confluent hypergeometric function [19], we obtain:

$$\frac{dS_{nl}(E)}{dE} = \left(\frac{n+l/2+1/2}{E} - \frac{1}{\hbar\Omega}\right)S_{nl}(E) - \frac{\sqrt{n(n+l+1/2)}}{E}S_{n-1,l}(E), \tag{31}$$

$$\frac{dC_{nl}(E)}{dE} = \left(\frac{n+l/2+1/2}{E} - \frac{1}{\hbar\Omega}\right)C_{nl}(E) - \frac{\sqrt{n(n+l+1/2)}}{E}C_{n-1,l}(E). \tag{32}$$

We note that $S_{nl}(E)$ and $C_{nl}(E)$ are two independent solutions of the second order finite-difference equation (7), and the Casorati determinant of these solutions,

$$\mathcal{K}_n(C,S) \equiv C_{n+1,l}(E)\, S_{n,l}(E) - C_{n,l}(E)\, S_{n+1,l}(E), \tag{33}$$

which plays the same role in the theory of linear difference equations as Wronskian in the theory of linear differential equations, differs from zero:

$$T^l_{n,n+1}\, \mathcal{K}_n(C,S) = \frac{q}{2}\hbar\Omega. \tag{34}$$

Using Eqs. (16), (31)–(34) we obtain

$$\left.\frac{d\,\delta_l(E)}{dE}\right|_{E=E_\nu} = \frac{q_\nu}{\hbar\Omega}\cdot\frac{1}{S^2_{N+1,l}(E_\nu)+C^2_{N+1,l}(E_\nu)} \times\left[\frac{2}{\langle N|\nu\rangle^2(N+1)(N+l+3/2)} - \frac{2}{q_\nu^2}\right], \tag{35}$$

where $q_\nu \equiv \sqrt{2E_\nu/\hbar\Omega}$. Expression (35) involves not only the eigenvalue E_ν but also the last component of the eigenvector $\langle N|\nu\rangle$. We would like to eliminate $\langle N|\nu\rangle$ in the expression for the derivative $\frac{d\,\delta_l(E)}{dE}$ at $E=E_\nu$.

The phase shift δ_l at $E=E_\nu$ in our approach is expressed through the function $f_{N+1,l}$ defined by Eq. (23). The function $f_{N+1,l}$ depends on the eigenenergy E_ν and the oscillator basis parameter $\hbar\Omega$, $f_{N+1,l} = f_{N+1,l}(E_\nu,\hbar\Omega)$. We recall that the value of E_ν depends on $\hbar\Omega$. Suppose that eigenvalue E'_ν is close enough to E_ν and the respective $\hbar\Omega'$ is close enough to $\hbar\Omega$. In this case, we have:

$$f_{N+1,l}(E'_\nu,\hbar\Omega') \simeq f_{N+1,l}(E_\nu,\hbar\Omega) + \frac{\partial f_{N+1,l}}{\partial E}(E'_\nu - E_\nu) + \frac{\partial f_{N+1,l}}{\partial\hbar\Omega}(\hbar\Omega' - \hbar\Omega). \tag{36}$$

The phase shift $\delta_l(E)$ depends only on the energy E and should not depend on $\hbar\Omega$. Therefore

$$\delta_l(E'_\nu) \simeq \delta_l(E_\nu) + \frac{d\delta_l}{dE}(E'_\nu - E_\nu). \tag{37}$$

The partial derivatives $\frac{\partial f_{N+1,l}}{\partial E}$ and $\frac{\partial f_{N+1,l}}{\partial\hbar\Omega}$ entering Eq. (36) can be calculated using Eqs. (23), (9) and (10), and then from Eqs. (35)–(37) we obtain

$$\frac{dE_\nu}{d\hbar\Omega} \simeq \frac{(E'_\nu - E_\nu)}{(\hbar\Omega' - \hbar\Omega)} \simeq \frac{1}{2}\langle N|\nu\rangle^2(N+1)(N+l+3/2). \tag{38}$$

Using Eq. (38), we rewrite the expression (35) as

$$\left.\frac{d\,\delta_l(E)}{dE}\right|_{E=E_\nu} \simeq \frac{q_\nu}{\hbar\Omega}\cdot\frac{1}{S^2_{N+1,l}(E_\nu)+C^2_{N+1,l}(E_\nu)}\left(\frac{1}{dE_\nu/d\hbar\Omega} - \frac{\hbar\Omega}{E_\nu}\right). \tag{39}$$

Since the phase shift derivative $\frac{d\delta_l(E)}{dE} > 0$ in the vicinity of resonance, it follows from Eq. (39) that

$$\frac{E_\nu}{\hbar\Omega} > \frac{dE_\nu}{d\hbar\Omega} > 0 \tag{40}$$

in the resonance region. If this inequality is not fulfilled, the eigenvalue E_ν corresponds to a non-resonant phase shift behavior.

One should be careful with using condition (40) for determining which of the Hamiltonian eigenstates obtained in a variational calculation with oscillator basis can be associated with a resonance. In such variational calculations, in the nuclear shell model in particular, each of the obtained eigenenergies usually decreases with $\hbar\Omega$ at small enough $\hbar\Omega$ values, gets a variational minimum at some $\hbar\Omega = \hbar\Omega_0$ and starts

increasing after this minimum. One should use only the increasing part of the function $E_\nu(\hbar\Omega)$ corresponding to $\hbar\Omega > \hbar\Omega_0$ for the analysis by means of inequality (40). The eigenvalues obtained at small $\hbar\Omega < \hbar\Omega_0$ before the minimum of $E_\nu(\hbar\Omega)$ may need strong so-called ultraviolet corrections [2, 3, 4] and thus lie outside ARJP. The $\hbar\Omega$ regions corresponding to large negative $\frac{dE_\nu}{d\hbar\Omega}$ cause the unphysical 'backbending' energy dependence of phase shift shown in the left panel of Fig. 2. Note also that in many-body calculations the energies $E_\nu(\hbar\Omega)$ should be calculated relative to the respective threshold. For example, in case of resonance associated with neutron scattered by nucleus ${}^AZ$, one should calculate the ground state energy $E_0^A(\hbar\Omega)$ and the energy $E_\nu^{A+1}(\hbar\Omega)$ of the state of interest in the nucleus ${}^{A+1}Z$ with respective oscillator quanta of excitations to obtain $E_\nu(\hbar\Omega)$ as

$$E_\nu(\hbar\Omega) = E_\nu^{A+1}(\hbar\Omega) - E_0^A(\hbar\Omega). \tag{41}$$

4 Breit–Wigner resonance

In a variational calculation with the oscillator basis with some truncation boundary N we obtain the energy E_ν of state ν as a function of oscillator parameter $\hbar\Omega$, $E_\nu = E_\nu(\hbar\Omega)$. As was shown above, using the function $E_\nu(\hbar\Omega)$, we can calculate the phase shifts $\delta_l(E)$ in some energy interval $[E_\nu(\hbar\Omega_1), E_\nu(\hbar\Omega_2)]$ where both $\hbar\Omega_1$ and $\hbar\Omega_2$ are within ARJP. Generally the interval $[E_\nu(\hbar\Omega_1), E_\nu(\hbar\Omega_2)]$ shifts down in energy and increases with N. If this energy interval includes a large enough slice of energy in the vicinity of some resonance, we can extract the resonance energy and width.

The phase shifts in the vicinity of resonance are conventionally described by the Breit–Wigner resonance formula [20],

$$\delta_l(E) = \arctan\left(\frac{\Gamma/2}{E_r - E}\right) - \phi_l, \tag{42}$$

where E_r and Γ are resonance energy and width respectively. The background phase ϕ_l is supposed to change only slightly in the resonance region, i. e., we can suppose $\phi_l = const$ in the vicinity of the resonance to obtain

$$\frac{d\delta_l}{dE} = \frac{\Gamma/2}{(E_r - E)^2 + (\Gamma/2)^2}. \tag{43}$$

The phase shift derivative $\frac{d\delta_l}{dE}$ gets its maximum at $E = E_r$. This maximal value of $\frac{d\delta_l}{dE}$ is related to the resonance width Γ:

$$\Gamma = 2\left(\frac{d\delta_l}{dE}\right)^{-1}\Bigg|_{E=E_r}. \tag{44}$$

Combining Eqs. (39) and (43), we obtain

$$\frac{\Gamma/2}{(E_r - E_\nu)^2 + (\Gamma/2)^2} = \frac{q_\nu}{\hbar\Omega} \cdot \frac{1}{S_{N+1,l}^2(E_\nu) + C_{N+1,l}^2(E_\nu)} \left(\frac{1}{dE_\nu/d\hbar\Omega} - \frac{\hbar\Omega}{E_\nu}\right). \tag{45}$$

This equation can be used directly for getting resonance parameters E_r and Γ from the fit to RHS of Eq. (45) where the function $E_\nu(\hbar\Omega)$ is obtained in variational calculations with oscillator basis with $\hbar\Omega$ values from ARJP. Having E_r and Γ one can easily obtain the background phase ϕ_l from Eq. (42) if some of the eigenenergies $E_\nu(\hbar\Omega)$ lie outside the resonance region.

We show in Fig. 6 the phase shifts supported by our model interaction (19) in the vicinities of resonances in s and d waves and their approximation in the vicinities of resonances by the Breit–Wigner formula (42) with parameters fitted using Eq. (45).

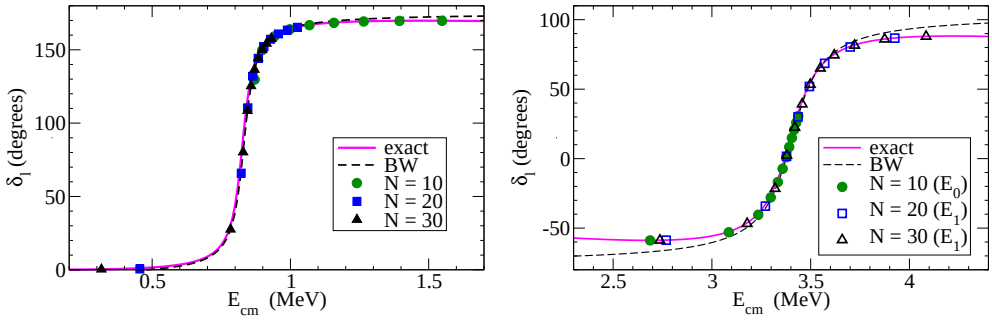

Figure 6: Phase shifts in the vicinity of resonances in d (left) and s (right) waves, resonance description by the Breit–Wigner formula with parameters E_r and Γ obtained by the fit using Eq. (45) and phase shifts used in this fit obtained by our approach [Eq. (21)] at eigenenergies $E_\nu(\hbar\Omega)$ calculated with various $\hbar\Omega$ values and truncations $N = 10$, 20 and 30. Filled symbols are the phase shifts obtained with the lowest eigenstates $E_0(\hbar\Omega)$, open symbols are the phase shifts obtained with the first excited eigenstates $E_1(\hbar\Omega)$.

The phase shifts at eigenenergies $E_\nu(\hbar\Omega)$ used in this fit are obtained with Hamiltonian truncations $N = 10$, 20 and 30 and are also depicted in Fig. 6. In the case of s wave, the lowest eigenstates $E_0(\hbar\Omega)$ lie below the resonant region, and we use the first excited states $E_1(\hbar\Omega)$ for the resonance parameter fit (the respective phase shifts are shown in Fig. 6 by open symbols). The Breit–Wigner formula is seen to nicely reproduce the phase shifts in the resonance region. The Breit–Wigner parameters obtained by the fit are: $E_r = 0.8315$ MeV, $\Gamma = 0.0602$ MeV and $\phi_l = 5°$ in the d wave and $E_r = 3.405$ MeV, $\Gamma = 0.230$ MeV and $\phi_l = 76°$ in the s wave. The fitted values of the resonance energies E_r and widths Γ reproduce with high precision the exact values given in Table 1.

The highly accurate description of the resonance parameters become possible because we use large enough truncation boundaries in calculations. It is also important to use a 'global' fit to a large enough set of eigenvalues $E_\nu(\hbar\Omega)$ covering the whole resonance region as the sets shown in Fig. 6. If we have restrictions in the size of the Hamiltonian, i. e., the values of N are not large enough, or the eigenvalues $E_\nu(\hbar\Omega)$ are available only at the edge of the resonance region, the quality of the fit is reduced.

We illustrate this statement by Fig. 7 where we demonstrate the results obtained with model interaction (19) with various truncations of the Hamiltonian. All results shown in this figure are obtained with eigenvalues $E_\nu(\hbar\Omega)$ fitting inequality (40) which are shown in the upper panels. The middle and lower panels demonstrate 'local' fits of resonance energies E_r and widths Γ, i. e., the fits utilizing only three neighboring eigenvalues $E_\nu(\hbar\Omega_{i-1})$, $E_\nu(\hbar\Omega_i)$ and $E_\nu(\hbar\Omega_{i+1})$ obtained with the same truncation N. We see that in the interval of $\hbar\Omega$ values where the eigenstates $E_\nu(\hbar\Omega)$ lie in the resonance region, the locally fitted resonance energies E_r and widths Γ form plateaus well reproducing the exact values. These plateaus are wider for larger N and for the lowest eigenstates $E_0(\hbar\Omega)$ than for excited eigenstates $E_1(\hbar\Omega)$. The plateaus for resonance energies E_r seem to be wider than for widths Γ; note however very different scales in the middle and lower panels. In the case of the s wave, the plateau for E_r is obtained even with a very small Hamiltonian truncated at $N = 5$. Note that a zigzag in E_r at $\hbar\Omega < 25$ MeV is due to the fact that these $\hbar\Omega$ values are outside ARJP for $N = 5$.

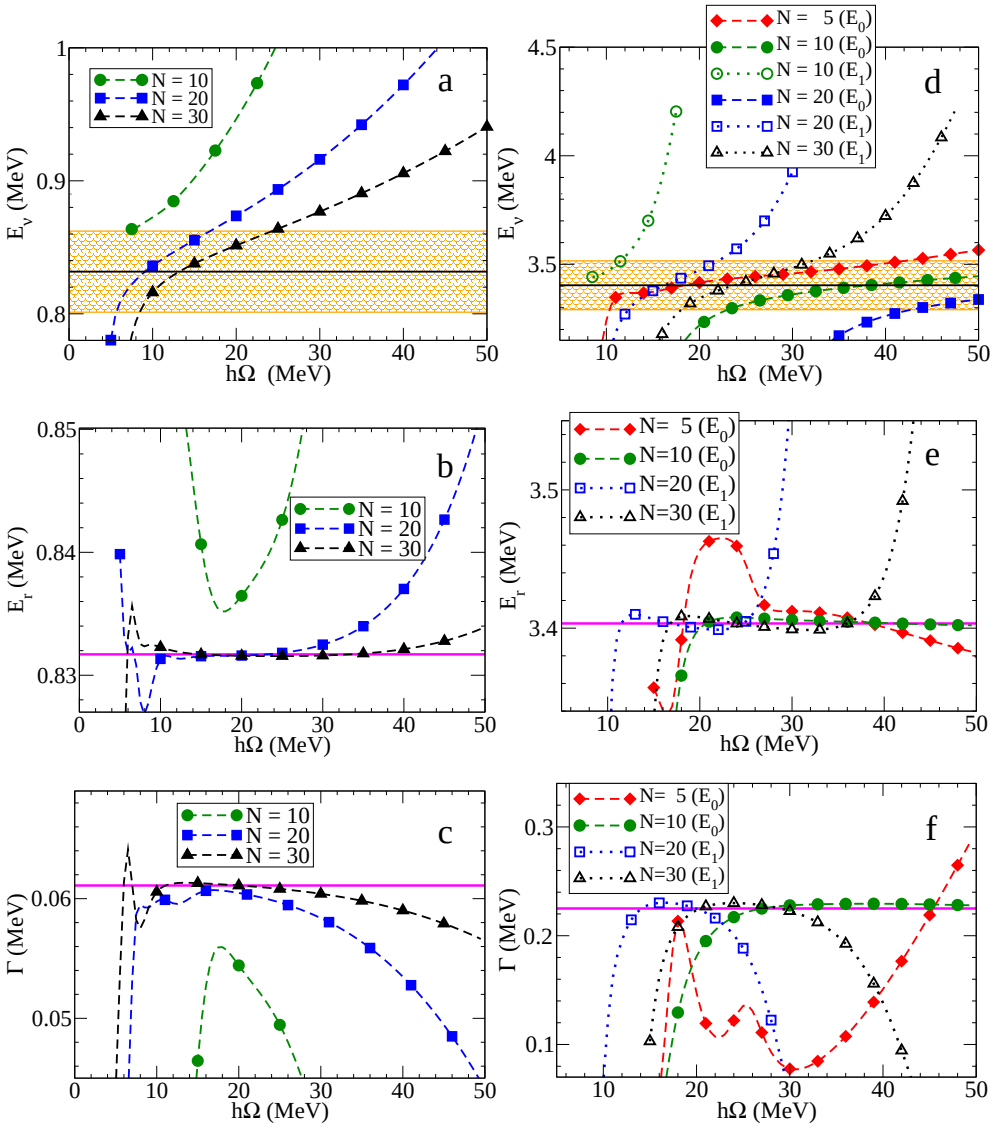

Figure 7: Eigenenergies E_ν (**a, d**) as functions of $\hbar\Omega$, resonance energies E_r (**b, e**) and widths Γ (**c, f**) obtained in 'local' fits (see text) with various truncations N for the d (left) and s (right) wave resonances. Solid lines depicts exact values of E_r and Γ, shaded areas in panels **a** and **d** show the resonance region. Filled symbols are the results for the lowest eigenstates $E_0(\hbar\Omega)$ while open symbols are the results for the first excited eigenstates $E_1(\hbar\Omega)$.

5 Analysis of resonant states in ^{5}He nucleus based on NCSM calculations

The suggested approach to extracting the resonance energy and width can be applied to any variational calculation with oscillator basis generating a set of eigenvalues $E_\nu(\hbar\Omega)$ forming a function of the oscillator basis spacing $\hbar\Omega$. As an example, we perform calculations of ^{5}He within NCSM [21] and analyze unbound states $3/2^-$ and $1/2^-$ in this nucleus. These states are observed as wide resonances in neutron scattering by α-particles; the $3/2^-$ resonance has an energy $E_r = 0.80$ MeV and width $\Gamma = 0.65$ MeV while the resonance parameters of the $1/2^-$ state

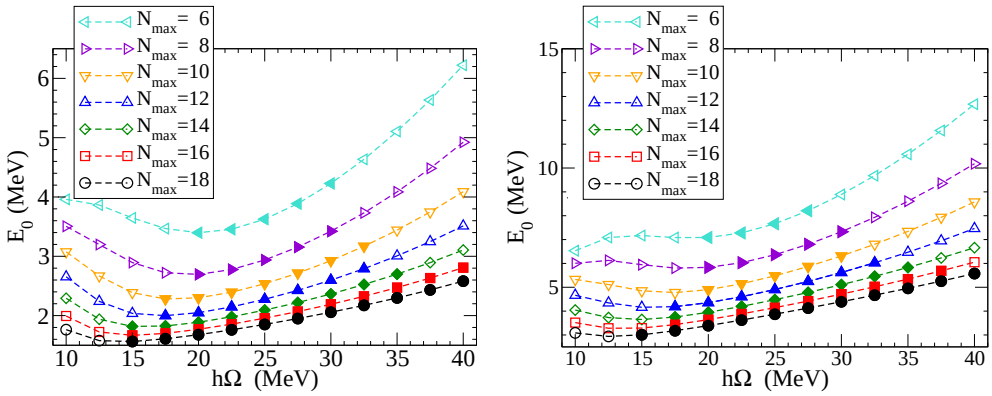

Figure 8: Energies $E_0(\hbar\Omega)$ of $n\alpha$ relative motion associated with $3/2^-$ (left) and $1/2^-$ (right) resonance states in ^{5}He obtained in NCSM calculations of ^{5}He and ^{4}He nuclei with various $N_{\max}$ truncations using JISP16 NN interaction. Filed (open) symbols depict eigenstates which fit (do not fit) inequality (40).

are $E_r = 2.07$ MeV and $\Gamma = 5.57$ MeV [22]. We use the JISP16 NN interaction [23] in our NCSM calculations. It is interesting to note that JISP16 and earlier versions of this type of NN interaction, ISTP [24] and JISP6 [25], arise from an application of J-matrix formalism to an inverse scattering treatment of the NN phase shift data.

A very important parameter of NCSM calculations is $N_{\max}$, maximal quanta of oscillator excitations included in the NCSM many-body basis space. It is easy to conclude that relation between the NCSM basis truncation $N_{\max}$ and the J-matrix truncation N associated with the principal quantum number of $n\alpha$ relative motion oscillator functions is $N_{max} = 2N$ in case of $3/2^-$ and $1/2^-$ states in ^{5}He.

The $3/2^-$ and $1/2^-$ resonances in ^{5}He are associated with the lowest eigenstates of respective spin-parity $\mathcal{E}^{(^5\mathrm{He},J^\pi)}_{N_{\max}}(\hbar\Omega)$ obtained in the NCSM calculations. Note however that we need for the analysis of resonance energy and width the energy $E_0(\hbar\Omega)$ of $n\alpha$ relative motion, i. e., the energy relative to the $n\alpha$ threshold given by Eq. (41) which in our case reads

$$E_0(\hbar\Omega) = \mathcal{E}^{(^5\mathrm{He},J^\pi)}_{N_{\max}}(\hbar\Omega) - \mathcal{E}^{(^4\mathrm{He},gs)}_{N_{\max}}(\hbar\Omega), \tag{46}$$

where $\mathcal{E}^{(^4\mathrm{He},gs)}_{N_{\max}}(\hbar\Omega)$ is the ^{4}He ground state energy obtained in NCSM with the same $N_{\max}$ and $\hbar\Omega$. The plots of energies $E_0(\hbar\Omega)$ obtained with various NCSM truncations $N_{\max}$ are shown in Fig. 8. Note, some of $n\alpha$ eigenstates $E_0(\hbar\Omega)$ do not fit inequalities (40) and cannot be used for calculations of resonance energy E_r and width Γ (they are shown by open symbols in Fig. 8).

We use only eigenstates $E_0(\hbar\Omega)$ to calculate phase shifts shown in Fig. 9. The borders of ARJP are unknown. We see that some phase shifts values obtained with different $N_{\max}$ truncations are in good correspondence and lie on the same curve. However we see that phase shifts calculated using few lowest eigenstates $E_0(\hbar\Omega)$ available for a given small enough basis spaces, i. e., basis spaces characterized by small enough $N_{\max}$ values, deviate essentially from the common curve. These smallest eigenstates correspond to lowest $\hbar\Omega$ values which evidently are outside the ARJP. The deviation from the common curve decreases as $N_{\max}$ increases. We should use for the calculation of Breit–Wigner parameters E_r and Γ only eigenstates $E_0(\hbar\Omega)$ providing the phase shifts forming the common phase shift curve and fitting inequalities (40), i. e., lying in the resonance region. As a result, we obtain $E_r = 1.41$ MeV and $\Gamma = 0.24$ MeV for the $3/2^-$ resonance and $E_r = 2.55$ MeV and $\Gamma = 0.91$ MeV for the $1/2^-$ resonance. The respective Breit–Wigner phase shifts are also shown in Fig. 9.

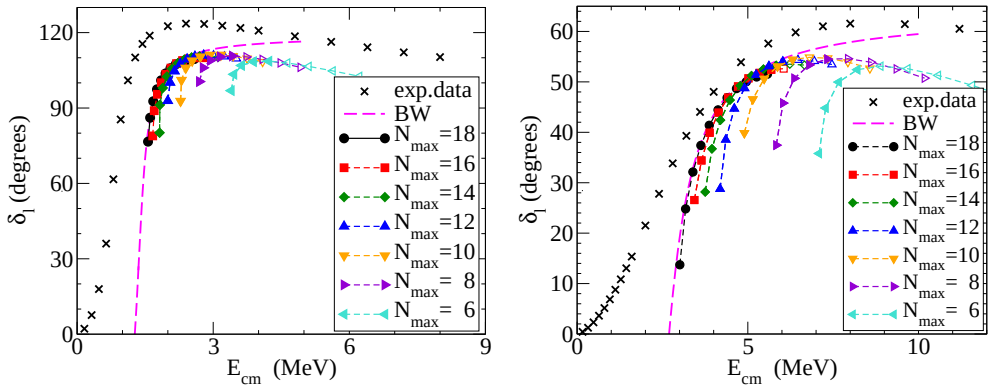

Figure 9: $n\alpha$ phase shifts in $3/2^-$ (left) and $1/2^-$ (right) states obtained by means of Eq. (21) using eigenstates $E_0(\hbar\Omega)$ depicted in Fig. 8 and Breit–Wigner phase shifts (42) calculated with E_r and Γ obtained by the fit. Filed (open) symbols correspond to eigenstates fitting (not fitting) inequality (40). Experimental data are taken from Ref. [26].

Our calculation overestimates resonance energies E_r and underestimates resonance widths Γ for both $3/2^-$ and $1/2^-$ resonances. This is clear from comparison with their experimental values ($E_r = 0.80$ MeV and $\Gamma = 0.65$ MeV for the $3/2^-$ resonance and $E_r = 2.07$ MeV and $\Gamma = 5.57$ MeV for the $1/2^-$ resonance) and from comparison of our phase shifts with experimental data of Ref. [26] shown in Fig. 9. The JISP16 interaction sifts the ^{5}He resonance states up in energy by about 0.5 MeV as compared to experiment. We note that the JISP16 interaction causes also underbinding of both ^{6}Li and ^{6}He nuclei by approximately 0.5 MeV [1]. This seems to be a drawback of the JISP16 interaction in description of nuclei at the beginning of p-shell which can be hopefully eliminated in future versions of this interaction by a more careful fit to experimental data which can include information about resonant states.

6 Conclusions

We formulated a simple method of accurate calculation of phase shifts which uses only eigenenergies E_ν obtained by diagonalization of the Hamiltonian in the oscillator basis and their dependence on the oscillator basis parameter $\hbar\Omega$. We analyze the relation of the suggested approach to other methods available in the literature. The method is illustrated by calculations of two-body scattering with model Woods–Saxon potentials.

Next we use this method to formulate an approach for calculating resonance energies and widths which can be applied to the analysis of results for energies above open thresholds obtained in any variational calculation with the oscillator basis, in the nuclear shell model in particular. We illustrate the accuracy of analysis of resonant parameters in calculations with model Woods–Saxon potentials and apply the suggested approach to calculation of resonances in $n\alpha$ scattering in NCSM with the JISP16 NN interaction.

The work was supported in part by the Ministry of Education and Science of Russian Federation through contract No 14.V37.21.1297 and by the US Department of Energy under Grant Nos. DE-FG02-87ER40371 and DESC0008485 (SciDAC-3/NUCLEI). This work was also supported in part by the National Science Foundation under Grant No PHY-0904782. A portion of the computational resources were pro-

vided by the National Energy Research Scientific Computing Center (NERSC), which is supported by the DOE Office of Science. AMS is also supported by the American Physical Society through the International Travel Grant Award Program.

References

[1] P. Maris, J. P. Vary and A. M. Shirokov, Phys. Rev. C **79**, 014308 (2009).

[2] S. A. Coon, M. I. Avetian, M. K. G. Kruse, U. van Kolck, P. Maris and J. P. Vary, Phys. Rev. C **86**, 054002 (2012).

[3] R. J. Furnstahl, G. Hagen, and T. Papenbrock, Phys. Rev. C **86**, 031301(R) (2012).

[4] S. N. More, A. Ekström, R. J. Furnstahl, G. Hagen and T. Papenbrock, Phys. Rev. C **87**, 044326 (2013).

[5] A. M. Shirokov, A. I. Mazur, J. P. Vary and E. A. Mazur, Phys. Rev. C **79**, 014610 (2009); A. M. Shirokov, A. I. Mazur, E. A. Mazur and J. P. Vary, Appl. Math. Inf. Sci. **3**, 245 (2009).

[6] G. Papadimitriou, J. Rotureau, N. Michel, M. Płoszajczak and B. R. Barrett, Phys. Rev. C **88**, 044318 (2013).

[7] G. Hupin, J. Langhammer, P. Navrátil, S. Quaglioni, A. Calci and R. Roth, arXiv:1308.2700 [nucl-th] (2013); S. Quaglioni, P. Navrátil, G. Hupin, J. Langhammer, C. Romero-Redondo and R. Roth, arXiv:1210.2020 [nucl-th] (2013).

[8] E. J. Heller and H. A. Yamany, Phys. Rev. A **9**, 1201 (1974); *ibid.* 1209 (1974).

[9] H. A. Yamany and L. Fishman. J. Math. Phys. **16**, 410 (1975).

[10] G. F. Filippov and I. P. Okhrimenko, Yad. Fiz. **32**, 932 (1980) [Sov. J. Nucl. Phys. **32**, 480 (1980)]; G. F. Filippov, Yad. Fiz. **33**, 928 (1981) [Sov. J. Nucl. Phys. **33**, 488 (1981)].

[11] Yu. F. Smirnov and Yu. I. Nechaev, Kinam **4**, 445 (1982); Yu. I. Nechaev and Yu. F. Smirnov, Yad. Fiz. **35**, 1385 (1982) [Sov. J. Nucl. Phys. **35**, 808 (1982)].

[12] V. A. Knyr, A. I. Mazur and Yu. F. Smirnov, Yad. Fiz. **52**, 754 (1990) [Sov. J. Nucl. Phys. **52**, 483 (1990)]; Yad. Fiz. **54**, 1518 (1991) [Sov. J. Nucl. Phys. **54**, 927 (1991)]; Yad. Fiz. **56**(10), 72 (1993) [Phys. At. Nucl. **56**, 1342 (1993)]; A. I. Mazur and S. A. Zaytsev, Yad. Fiz. **62**, 656 (1999) [Phys. At. Nucl. **62**, 608 (1999)].

[13] V. I. Kukulin, V. N. Pomerantsev and O. A. Rubtsova, JETP Lett. **90**, 402 (2009); O. A. Rubtsova, V. I. Kukulin, V. N. Pomerantsev and A. Faessler, Phys. Rev. C **81**, 064003 (2010).

[14] I. M. Lifshitz, Zh. Eksp. Teor. Fiz. **17**, 1017 (1947) (*in Russian*); *ibid.* **17**, 1076 (1947) (*in Russian*); Usp. Mat. Nauk **7**, 171 (1952) (*in Russian*).

[15] J. M. Bang, A. I. Mazur, A. M. Shirokov, Yu. F. Smirnov and S. A. Zaytsev, Ann. Phys. (NY) **280**, 299 (2000).

[16] A. M. Shirokov, A. I. Mazur, S. A. Zaytsev, J. P. Vary and T. A. Weber, Phys. Rev. C **70**, 044005 (2004).

[17] J. Revai, M. Sotona and J. Žofka, J. Phys. G **11**, 745 (1985).

[18] A. M. Shirokov, Yu. F. Smirnov and S. A. Zaytsev, in *Modern problems in quantum theory*, edited by V. I. Savrin and O. A. Khrustalev. Moscow, 1998, p. 184; Teoret. Mat. Fiz. **117**, 227 (1998) [Theor. Math. Phys. **117**, 1291 (1998)].

[19] M. Abramowitz and I. A. Stegun (eds.), *Handbook on mathematical functions*. Dover, New York, 1972; NIST Digital Library of Mathematical Functions, http://dlmf.nist.gov/.

[20] A. M. Lane and R. G. Thomas, Rev. Mod. Phys. **30**, 257 (1958).

[21] P. Navrátil, J. P. Vary and B. R. Barrett, Phys. Rev. Lett. **84**, 5728 (2000); Phys. Rev. C **62**, 054311 (2000).

[22] A. Csótó and G. M. Hale, Phys. Rev. C **55**, 536 (1997).

[23] A. M. Shirokov, J. P. Vary, A. I. Mazur and T. A. Weber, Phys. Lett. B **644**, 33 (2007).

[24] A. M. Shirokov, A. I. Mazur, S. A. Zaytsev, J. P. Vary and T. A. Weber, Phys. Rev. C **70**, 044005 (2004).

[25] A. M. Shirokov, J. P. Vary, A. I. Mazur, S. A. Zaytsev and T. A. Weber, Phys. Lett. B **621**, 96 (2005); J. Phys. G **31**, S1283 (2005).

[26] J. E. Bond and F. W. K. Firk, Nucl. Phys. A **287**, 317 (1977).